

Chapter 3

Materials and Experimental Procedure

3.1 Introduction

This chapter offers a comprehensive overview of the materials and synthesis methods used for synthesis of high entropy oxides (HEOs), along with the post-annealing processes. It also provides a concise description of the characterization techniques and analytical methods employed, including X-ray diffraction (XRD), X-ray photoelectron spectroscopy (XPS), FE-SEM, UV-Vis, spectroscopy, Electrochemical impedance spectroscopy (EIS), and a range of other spectroscopy techniques.

3.1.1 Solution combustion synthesis

To synthesize high entropy oxides, we utilized solution combustion synthesis technique. SCS is a self-sustaining chemical process that unfolds in a homogeneous solution of precursors [119,187,188]. SCS begins with dehydration and thermal decomposition, setting off a cascade of thermally coupled exothermic reactions. These reactions culminate in the fabrication of at least one solid product and a significant release of gases. Solution combustion synthesis, along with other combustion synthesis methods, operates in two distinct modes. One such mode is known as volume combustion or thermal explosion. In this approach, the entire reactive mixture is uniformly preheated to the solvent's boiling point (Stage I). This

initiates a relatively prolonged phase at a constant temperature (Stage II), during which free and some bound water evaporates [187]. Subsequently, the system enters a more rapid preheating phase (Stage III), which accelerates until reaching the ignition temperature (T_{ig}). At this critical point, the temperature surges to a maximum value (T_m) (Stage IV) followed by the final cooling phase (Stage V). This processing highlights the dynamic thermal nature of the SCS process, crucial for material synthesis. **Figure 3.1** showing a schematic representation of SCS [189]. The second mode of solution combustion synthesis is known as the self-propagating combustion mode, where the reaction progresses through the mixture in the form of a combustion wave. Unlike volume combustion, this mode features a much shorter preheating stage, making it a faster and more dynamic process for synthesizing materials. Several heating methods can initiate the solution combustion synthesis process, each defining a unique pathway for the reaction.

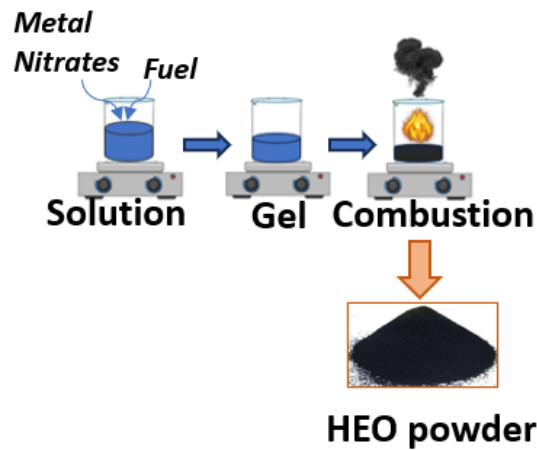


Figure 3.1 Schematic depicts solution combustion synthesis.

The simplest and most widely used technique involves placing a glass or ceramic container with the precursor solution on a hot plate or in a preheated furnace,

typically maintained at 200–300 °C. This straightforward approach seamlessly integrates heating, solvent evaporation, gel formation and decomposition, self-ignition, combustion, and solid product formation into a single technological step, making it highly efficient and accessible for SCS applications [29,65,190]. SCS is carried out in an aqueous solution of an oxidizer and a fuel, which generates sufficient exothermic energy to sustain a self-propagating chemical reaction. Common oxidizers are hydrated metal nitrates, while fuels such as urea, glycine, and citric acid play a dual role: they not only provide the heat required for the reaction but also form stable complexes with metal ions [191,192], enhancing their solubility and preventing selective precipitation during water removal. SCS operates through a self-sustained redox reaction between oxidizers and fuels, thoroughly mixed at the molecular level. This reaction is driven by the system's natural tendency to reduce its Gibbs free energy (ΔG), converting chemical potential into heat. Under adiabatic conditions, energy and mass exchange with the environment are negligible and the initial reactive solution remains stable at low temperatures without significant changes in composition, temperature, or pressure. However, this quasi-stationary state is inherently unstable. When the system temperature reaches a critical reaction onset point, exothermic reactions ignite, generating heat that accelerates the reaction rate in a self-sustaining cycle. The process concludes when all reactants are transformed into products, and the system attains a new equilibrium state, where ΔG is minimized. This dynamic process can be understood as a transition from an initial non equilibrium quasi-stationary state at which ΔG is not at its minimum to a final equilibrium steady state [60,119,193,194]. During combustion, the system rapidly releases energy, driving

the reaction to completion. Although the system exchanges heat with its surroundings over longer timescales (10-100 seconds), the resulting material reaches ambient temperature and achieves thermodynamic equilibrium, completing the synthesis process.

3.2 Preparation for deposition

3.2.1 Materials

Cobalt (II) nitrate hexahydrate $\text{Co}(\text{NO}_3)_2 \cdot 6\text{H}_2\text{O}$, copper nitrate trihydrate $\text{Cu}(\text{NO}_3)_2 \cdot 3\text{H}_2\text{O}$, nickel nitrate hexahydrate $\text{Ni}(\text{NO}_3)_2 \cdot 6\text{H}_2\text{O}$, magnesium nitrate hexahydrate $\text{Mg}(\text{NO}_3)_2 \cdot 6\text{H}_2\text{O}$, zinc nitrate hexahydrate $\text{Zn}(\text{NO}_3)_2 \cdot 6\text{H}_2\text{O}$, and calcium nitrate tetrahydrate $\text{Ca}(\text{NO}_3)_2 \cdot 4\text{H}_2\text{O}$, lithium nitrate $\text{Li}(\text{NO}_3)$, sodium nitrate $\text{Na}(\text{NO}_3)$, iron nitrate nonahydrate $\text{Fe}(\text{NO}_3)_3 \cdot 9\text{H}_2\text{O}$ were purchased from Merk Inc. (purity assay $\sim 99\%$) and used without any further purification. These metal nitrates were utilized to synthesize nanocrystalline HEOs powder. The calculated amount of metal nitrates was dissolved in distilled water, followed by mixing an appropriate amount of citric acid ($\text{C}_6\text{H}_8\text{O}_7$) at room temperature. The solution formed was stirred continuously for 24 hours at 80°C using a magnetic stirrer. The pH of the solution was adjusted to 7 using 30% ammonia solution, forming a dark blue gel. Subsequently, the temperature was raised slowly to range of 523-623 K when the combustion reaction was ignited, resulting in the formation of nanocrystalline powders. **Figure 3.2** illustrate the procedure for synthesis of HEOs using SCS method. However, all the compositions did not yield a single-phase solid solution and were further annealed to required higher temperatures to obtain a single-phase rocksalt HEO. The thesis began with the low-temperature

synthesis of (Mg,Co,Ni,Cu,Zn)O rocksalt high entropy oxides, followed by isovalent (Ca^{2+}) and aliovalent (Fe^{3+} , Li^+ , and Na^+) cation addition in (Mg,Co,Ni,Cu,Zn)O. Each composition requires different annealing temperature for single phase formation. Therefore, the processing details and specific composition is discussed in the relevant chapters.

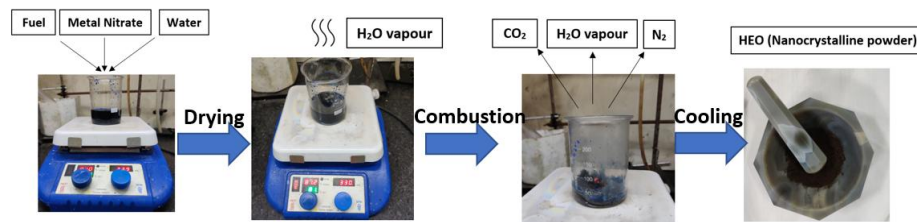


Figure 3.2 Synthesis of HEO powder using solution combustion synthesis (SCS).

3.3 Characterization techniques

3.3.1 X-ray diffraction

X-ray diffraction is one of the most commonly used technique for identifying crystallographic phases and determining structural parameters such as d-spacing and lattice constants. In a typical X-ray diffraction experiment, an X-ray beam is directed onto a specimen and scattered by its atoms. The intensity of the elastically scattered X-rays is influenced by the atomic mass and the long-range arrangement of atoms within the material.

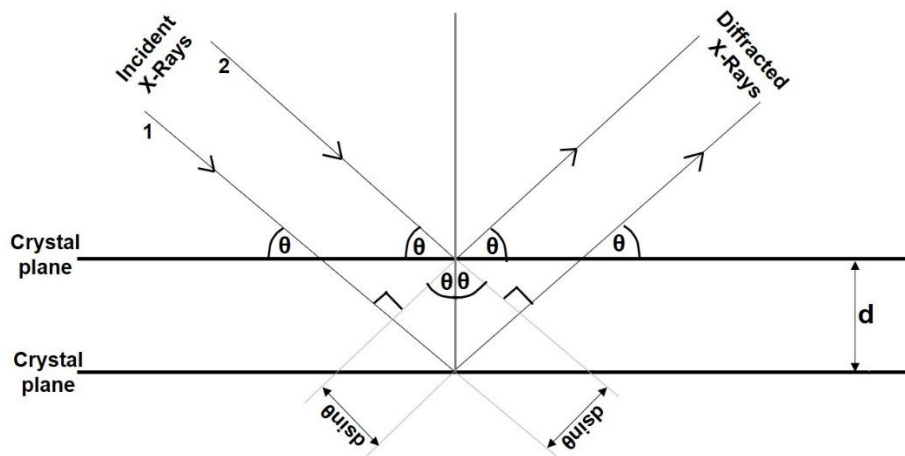


Figure 3.3 Schematic diagram of Bragg's law.

Due to this arrangement, the scattered beams are in phase in specific directions, leading to constructive interference and the formation of diffraction peaks corresponding to the d-spacing of the crystallographic planes. This phenomenon is described by Bragg's law; which states that, constructive interference and hence a diffraction peak occurs when an X-ray beam strikes a crystal surface at an angle θ , satisfying Bragg's condition. The mathematical expression of Bragg's law is shown in Equation 1 and illustrated in **Figure 3.3**

$$n\lambda = 2d \sin\theta \quad (1)$$

By examining the angles of the diffraction peaks, the corresponding d-spacing for the diffracting planes can be determined with ease. Additionally, the crystallite size (t) can be estimated using the Scherrer equation.

$$t = \frac{0.9\lambda}{B \cos \theta_B} \quad (2)$$

where the width B is the full-width at half maxima (FWHM) of the diffraction peak, usually measured in radians, at an intensity equal to half the maximum intensity, λ is the wavelength of X-rays Cu-K α (1.54056 Å), and θ_B is the XRD peak position. X-ray diffraction patterns of the various composition of HEO were recorded utilizing a diffractometer Rigaku Mini Flex-600 (40 kV-15 mA); Rigaku, Tokyo, Japan using Cu-K α radiation ($\lambda=1.54056$ Å). The data were recorded in 2θ scan range from 20 to 80° at a step size of 0.02°, while the scan rate was 2°/min.

3.3.2 Thermogravimetric analysis

The Thermogravimetric Analysis (TGA) technique measures changes in the mass of a sample as it is heated, cooled, or held at a constant temperature over time. This powerful method unravels both physical phenomena like phase transitions, absorption, and desorption and chemical processes, including chemisorption, thermal decomposition, and solid-gas interactions. A typical thermogravimetric analyzer (TGA) comprises a high-precision balance and a sample pan enclosed within a temperature-controlled furnace. The furnace allows programmable temperature changes, either at a constant rate or tailored for specific mass loss requirements, to drive thermal reactions. **Figure 3.4** shows the photograph of TGA. These reactions can occur under diverse conditions, including ambient air, inert or reactive gases (oxidizing, reducing, or corrosive), liquid vapors, or even self-generated atmospheres, across a wide range of pressures from high vacuum to high-pressure environments. The data gathered from TGA experiments is presented as a plot of mass (or percentage of initial mass) versus temperature or time, known as the TGA curve.



Figure 3.4 Photograph of typical thermogravimetric analyzer (TGA).

3.3.3 Differential thermal analysis

Differential Thermal Analysis (DTA) is a technique used to measure temperature differences between a sample and an inert reference material as they are subjected to the same thermal conditions. The setup involves placing both the sample and reference in separate pans within a furnace equipped with thermocouples to monitor

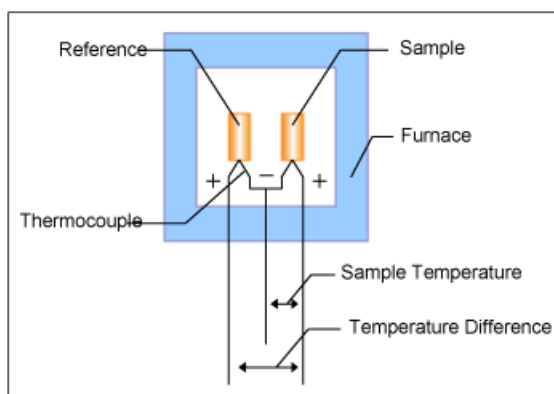


Figure 3.5 Depicts the schematic of Differential Thermal Analysis (DTA).

their temperatures. While the reference remains thermally stable, the sample undergoes thermal events such as phase transitions or chemical reactions, causing its temperature to deviate from that of the reference. These deviations are recorded

as a function of temperature or time. **Figure 3.5** shows the schematic of DTA. Endothermic processes, such as melting or dehydration, result in a temperature lag, while exothermic processes, like crystallization or oxidation, cause the sample temperature to rise above the reference. The resulting DTA curve reveals peaks corresponding to these events, with downward peaks indicating endothermic reactions and upward peaks for exothermic ones. By analyzing the position and area of these peaks, DTA provides qualitative and semi-quantitative insights into phase transitions, decomposition, and reaction kinetics. In our work the differential thermal analysis (DTA) and thermogravimetric analysis (TGA) (EXSTAR TG/DTA 6300) were carried out in the air (flow rate 200 ml/min) at 5 °C/min from 25 °C to 1000 °C.

3.3.4 Differential scanning calorimetry

Differential Scanning Calorimetry (DSC) is a thermal analysis technique that measures the heat flow associated with thermal transitions in a material under controlled temperature conditions. A sample and an inert reference are placed in separate pans, and their heat flow is monitored as the temperature is increased, decreased, or held constant.



Figure 3.6 Photograph of Differential Scanning Calorimetry (DSC).

Thermal events such as melting, crystallization, or chemical reactions cause differences in heat flow, with endothermic processes absorbing energy and exothermic processes releasing it. The resulting DSC curve provides information on transition temperatures and reaction enthalpies, making it an essential tool in thermal analysis. Differential scanning calorimetry (DSC) (Shimadzu (Asia Pacific) Pte Ltd. Model-DSC-60, USA, (**Figure 3.6**) set up calibrated with 10 mg of alumina) was carried out by heating the samples in air (100 ml/min) at 10 °C/min from 25 to 420 °C.

3.3.5 Fourier transform infrared spectroscopy

The working principle of Fourier Transform Infrared (FTIR) spectroscopy relies on the absorption of infrared (IR) radiation by a sample, causing molecular vibrations. In an FTIR spectrometer, a broad-spectrum IR radiation source directs light toward the sample. The light passes through an interferometer, where it is split into two beams: one reflecting off a stationary mirror and the other off a moving mirror. These beams recombine, creating an interference pattern known as an interferogram. As the IR beam interacts with the sample, specific wavelengths are

absorbed by the sample's molecules based on their vibrational frequencies, while the remaining radiation passes through. The detector captures the modified IR beam, and the resulting data, which contains absorption information, is subjected to a Fourier Transform. This mathematical process converts the raw data into an IR spectrum, displaying absorbance or transmittance versus wavenumber. The peaks in the spectrum correspond to specific molecular vibrations and functional groups,



Figure 3.7 Photograph of Fourier transform infrared spectroscopy (FTIR).

allowing for the identification of organic, polymeric, and, in some cases, inorganic materials. **Figure 3.7** showing the photograph of FTIR. In our work the Fourier transform infrared spectroscopy (FTIR (Model-Tensor II, Bruker, USA) was carried out.

3.3.6 Field emission scanning electron microscopy

Field emission scanning electron microscopy (FESEM) is an advanced technique for studying the microstructure and elemental composition of materials. It employs an electron gun to generate an electron beam with energies ranging from a few hundred eV to a few keV. This beam is focused into a fine probe, typically less than 5 nm in diameter, using electromagnetic lenses. The sample surface is scanned by raster the electron beam across it.

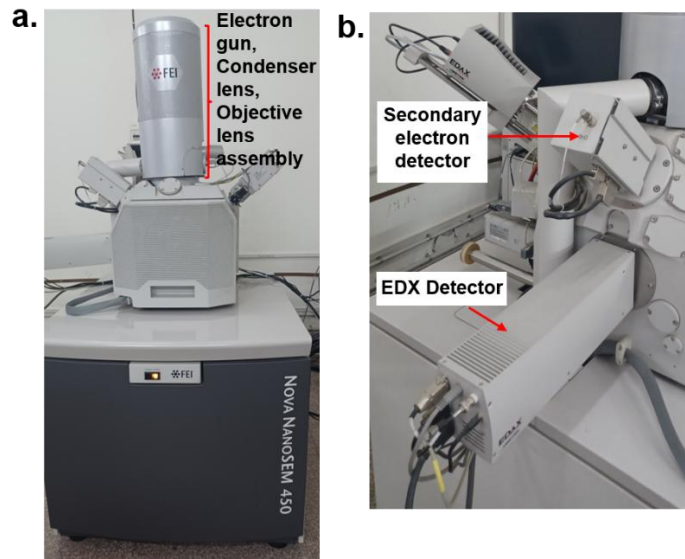


Figure 3.8 (a) Front view of FESEM (b) Side view of FESEM.

The FESEM model Nova Nano SEM 450, supplied by FEI Inc (S.E.A. PTE LTD, USA) as shown in **Figure 3.8** a was utilized for imaging ZnO, AZO, Tl-Al-ZnO films, while the energy-dispersive X-ray spectra of the films were acquired using a customary unit (Pegasus Integrated EDS-EBSD with Octane Plus and Hikari Pro, EDAX Inc.) attached to the FESEM as shown in **Figure 3.8b**. Within the specimen, high-energy electrons undergo elastic and inelastic interactions, producing various signals such as secondary electrons, backscattered electrons, characteristic X-rays, continuous X-rays, and Auger electrons. FESEM primarily utilizes secondary and backscattered electrons for imaging. Secondary electrons, being low-energy, are surface-sensitive and provide fine details of the surface topology. Backscattered electrons, with higher energy, reveal compositional contrasts in the specimen. Additionally, energy dispersive X-ray spectroscopy (EDX), often integrated with FESEM, identifies the elemental composition of the material by analyzing emitted characteristic X-rays.

3.3.7 Transmission electron microscopy

Transmission Electron Microscopy (TEM) is a powerful analytical technique extensively used to investigate the microstructure, crystallography, and chemical composition of materials at nanometer and even atomic resolutions. By employing a highly focused electron beam that passes through an ultra-thin sample, TEM provides unparalleled insights into the internal structure of materials. This capability makes it an indispensable tool in materials science, nanotechnology, and related fields. TEM operates on the principle of electron transmission, where electrons with high kinetic energy (typically 80–300 keV) interact with the sample. As the electrons traverse the material, they undergo scattering, producing a range of transmitted, diffracted, and inelastically scattered electrons. These interactions form the basis for generating various imaging and analytical data, including high-resolution images, diffraction patterns, and elemental maps. A significant advantage of TEM is its versatility, allowing for the study of structural details such as grain boundaries, defects, and crystallographic orientations, as well as the elemental and chemical states of a material. Advanced TEM techniques, including high-resolution TEM (HRTEM), selected area electron diffraction (SAED), scanning TEM (STEM), and energy dispersive X-ray spectroscopy (EDS), further enhance its capabilities for nanoscale characterization. The combination of high spatial resolution, chemical analysis, and crystallographic information makes TEM a cornerstone technique in the exploration of material properties and the correlation of their structure with functionality.



Figure 3.9 High resolution transmission electron microscope (HR TEM).

Transmission electron microscopy images and selected area diffraction pattern (SAED) were recorded by TEM (Tecnai G2 20 TWIN, FEI) under an operating voltage of 200 kV (**Figure 3.9**). Samples for TEM imaging were prepared by dispersing the powder in ethanol through ultrasonication for 60-80 min followed by drop-casting on a 200-mesh carbon-coated Cu grid.

3.3.8 X-ray photoelectron spectroscopy

When X-ray photons strike a sample, electrons within the material absorb the photon energy and are ejected from the sample. The kinetic energy of these emitted electrons is measured using a hemispherical analyzer. The hemispherical analyzer consists of two concentric, conductive hemispheres maintained at different potentials. Electrons with kinetic energies within the analyzer potential difference follow a specific trajectory through the hemispheres and are ultimately collected at the detector. **Figure 3.10a** shows the various component of XPS. The trajectory varies depending on the electrons' kinetic energy, enabling the analyzer to map

kinetic energies to positions on the detector. To scan a range of kinetic energies, the analyzer potential is varied continuously while maintaining a constant pass energy, ensuring consistent resolution. The kinetic energy of electrons escaping from the surface depends on the incident energy and binding energy of the escaping electron. From the law of the conservation of energy, BE can be given as

$$BE = hv - KE - \phi \quad (3)$$

where hv is the energy of the photon, KE is the kinetic energy of the knocked-out electron, and ϕ is the work function of the spectrometer. The binding energy of electrons provides critical information about their elemental origin and oxidation state, while the relative intensity of the peaks can be used to determine the elemental concentrations. XPS enables the determination of elemental composition, empirical formula, and chemical oxidation states of elements in a sample. For this study, XPS measurements were conducted using a Thermo Scientific Nexsa XPS system equipped with a double-focusing hemispherical analyzer and a 128-channel detector, as illustrated in **Figure 3.10b**. The X-ray source was an Al-K α gun with an energy of 1486 eV. The binding energy scale was calibrated using the adventitious carbon C1s peak at 284.8 eV. A pass energy of 20 eV was used for elemental analysis, while a pass energy of 200 eV was employed during the survey scan.

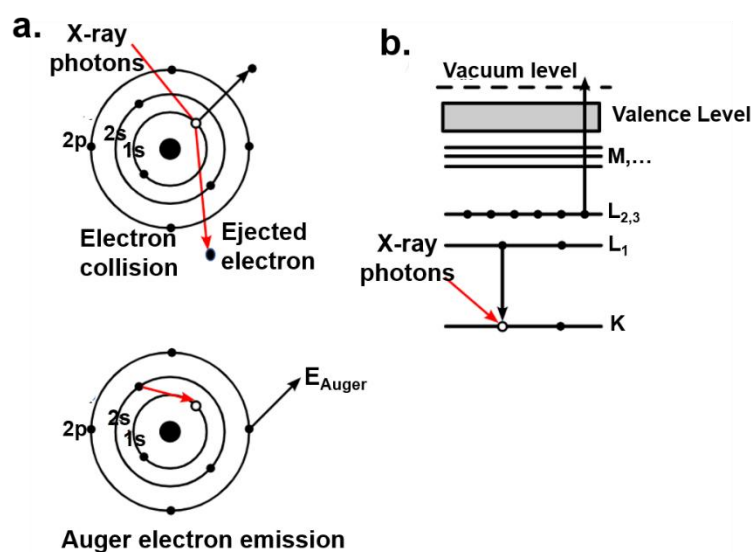


Figure 3.10 (a) schematic representation of Auger electron emission, and (b) Auger electron emission in X-ray notation ($KL_1L_{2,3}$).

In addition to XPS peaks, Auger peaks are observed in XPS spectra due to electron transitions. These occur when the energy released during the filling of an inner core-shell vacancy is sufficient to eject an outer-shell electron, as illustrated in **Figure 3.10(a,b)**. The "modified" Auger parameter (β') is defined as the sum of the binding energy (BE) of the most intense photoelectron peak and the kinetic energy (KE) of its corresponding Auger peak. When photoelectron peaks show less chemical shift, the relative movement of the Auger peak to the photoelectron peak can help determine the chemical state of the atoms. A higher Auger parameter corresponds to a lower oxidation state of the element, while a lower Auger parameter indicates a higher oxidation state.

3.3.9 UV-VIS spectroscopy

Ultraviolet-visible (UV-Vis) spectroscopy is an analytical tool widely used in laboratories globally for its simplicity and versatility. This technique utilizes the ultraviolet and visible regions of the electromagnetic (EM) spectrum, with the UV range spanning 100-400 nm and the visible range covering approximately 400-800 nm. When radiation interacts with matter, various phenomena can occur, such as reflection, scattering, absorbance, fluorescence/phosphorescence (absorption and re-emission), and photochemical reactions. Typically, absorbance measurements are performed to obtain the UV-Vis spectrum of a sample. The semiconductor bandgap can then be determined from the absorption data using a Tauc plot. The energy-dependent absorption co-efficient estimated by the following relation

$$(\alpha \cdot hv)^{1/\gamma} = B(hv - E_g) \quad (4)$$

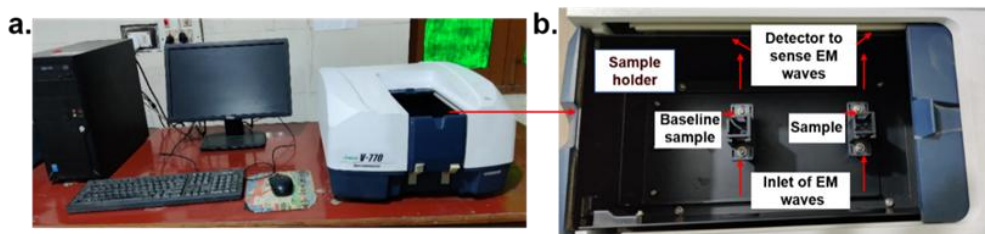


Figure 3.11 (a) Photograph of UV VIS spectroscopy setup and, (b) Photograph of the sample holder chamber.

where α is the absorption coefficient, hv is the incident photoenergy, and E_g is the optical bandgap, while γ is a factor that has values 2 or $\frac{1}{2}$ for the indirect or direct nature of electron transition, respectively. A UV-Vis spectrometer (JASCOW-770,

USA, shown in **Figure 3.11 (a,b)** was used to identify the bandgap and measure absorbance, of various compositional HEOs powder.

3.3.10 Surface area measurement using Brunauer-Emmett Teller (BET) method

The Brunauer-Emmett-Teller (BET) method is a widely used technique for characterizing the surface area and porosity of materials, particularly powders, catalysts, and porous solids. Developed in 1938 by Stephen Brunauer, Paul Emmett, and Edward Teller, the BET method is based on the physical adsorption of gas molecules onto the surface of a material, providing key insights into the material's surface area, pore size distribution, and surface chemistry. The BET method operates on the principle that gas molecules, when exposed to a solid surface under specific conditions (usually low temperatures), will adsorb onto the surface. As the pressure of the adsorbate gas increases, additional layers of gas molecules can be adsorbed. The BET theory extends the Langmuir adsorption model, which assumes monolayer adsorption, to include multilayer adsorption. **Figure 3.12** showing the photograph of BET instrument. The BET method provides valuable information on the specific surface area of a material, typically expressed in terms of square meters per gram (m^2/g). This surface area is crucial for understanding the material's reactivity, catalytic properties, and adsorption capacity, among other characteristics. In addition to surface area,



Figure 3.12 (a) Photograph of BET instrument.

BET analysis can also provide insights into porosity and pore size distribution. When adsorption isotherms are measured at different relative pressures, the data can reveal information about the size and distribution of pores within the material, allowing for the characterization of mesoporous and microporous materials. These measurements are particularly useful for catalysts, adsorbents, and materials used in energy storage applications. In our work surface area measurements were performed by nitrogen adsorption at 77 K (BET, Bellsorp Max ii & Belcat-ii) using the Brunauer-Emmett-Teller (BET) method.

3.3.11 X-ray absorption spectroscopy

X-ray absorption spectroscopy (XAS) is a powerful, element-specific technique that leverages the photoelectric effect. The primary physical process in X-ray absorption involves the absorption of a photon, which ejects a core-level photoelectron from the absorbing atom, leaving behind a core hole. As a result, the atom with the core hole becomes excited, and the ejected photoelectron interacts with the surrounding atoms as shown in **Figure 3.13**. If the ejected photoelectron is treated as a wave and the surrounding atoms are modeled as point scatterers, the

backscattered electron waves can interfere with the forward-propagating waves. This interference creates a modulation in the absorption coefficient, leading to the oscillations observed in EXAFS spectra. When monochromatic X-rays with energy E pass through a homogeneous sample of thickness x , get absorbed according to the Beer-Lambert law.

$$I_t(E) = I_0(E)e^{-\mu(E)x} \quad (5)$$

This relationship connects the incident intensity $I_0(E)$ and the transmitted intensity $I_t(E)$ as where $\mu(E)$ is the linear X-ray absorption coefficient and x is thickness of sample. X-ray photons with energies capable of exciting core-level electrons (1s, 2s, or 2p) are typically used in X-ray Absorption Spectroscopy (XAS) to reveal structural information. For transition metals and heavier elements, upper-level electrons (3s, 3p, 3d, etc.) can also be probed to explore the local electronic structure. The spectra are classified by absorption edges K, L, M, and so on corresponding to the principal quantum numbers $n=1,2,3$ respectively.

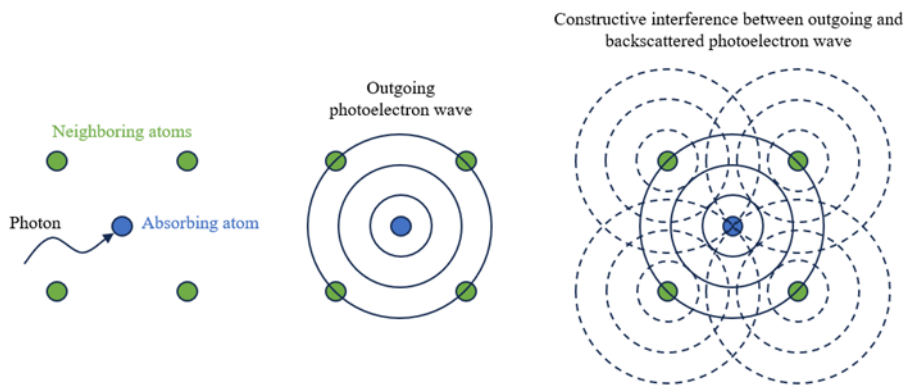


Figure 3.13 Schematic representation of scattering of core electron of absorbing atom to electron wave of neighbouring atom.

XAS is governed by electric dipole selection rules ($\Delta l = \pm 1$), with each edge revealing unique transitions:

- K-edge: $1s \rightarrow$ empty np states
- L1-edge: $2s \rightarrow$ empty np states
- L2-edge: $2p_{1/2} \rightarrow$ empty $nd_{3/2}$ states
- L3-edge: $2p_{3/2} \rightarrow$ empty $nd_{3/2}$ and $nd_{5/2}$ states

While transitions from 2p to ns states are allowed, they exhibit weak intensity and are often overlooked. The electron ejected by the X-ray photon, known as the photoelectron, requires a minimum energy (E_0) equal to its binding energy to be freed from the atom. This threshold energy marks the starting point for unraveling the electronic and structural intricacies of materials. The X-ray Absorption Spectroscopy spectrum is divided into two key regions as shown in **Figure 3.14**.

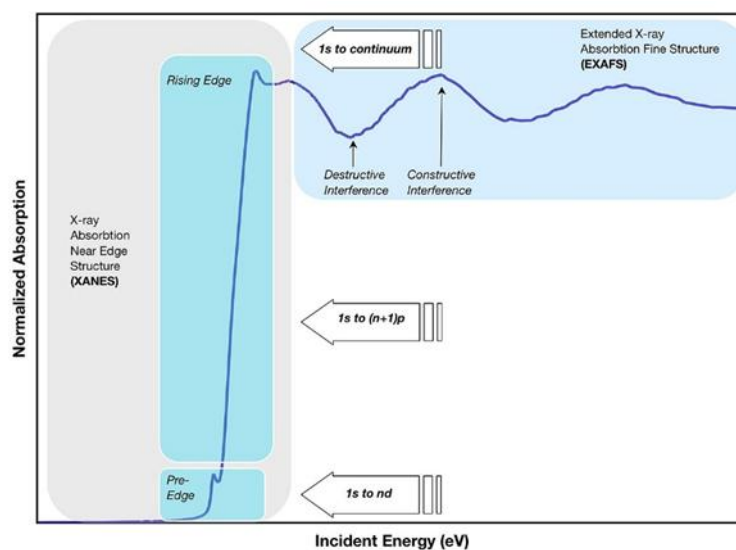


Figure 3.14 Illustrate three regions in X-ray absorption spectroscopy (XAS).

X-ray absorption near edge spectroscopy (XANES)

Spanning approximately 10 eV below to 20 eV above the absorption edge, XANES provides critical insights into the oxidation state and local symmetry or coordination environment of the targeted element. It also offers information about the unoccupied electronic density of states above the Fermi level, making it invaluable for probing electronic and chemical properties.

Extended X-ray absorption fine structure (EXAFS)

Starting about 50 eV above the edge, EXAFS reveals details about the short-range atomic structure surrounding the absorption atom. It provides information on the identity of neighbouring atoms, their distances from the central atom, and the coordination number, i.e., the number of nearest neighbours. Together, XANES and EXAFS deliver a comprehensive picture of both the electronic and local structural

environment of the element under investigation. The fine structure of the synthesized powders was studied using X-ray absorption spectroscopy. EXAFS and XANES were performed at INDUS 2 synchrotron facility (Raja Ramanna Centre for Advanced Technology, Indore, India). The X-ray absorption spectra were recorded across the K-absorption edges of Co, Cu, Ni, and Zn using an ionization chamber. K-edge absorption energies were aligned using the metal foil of each element. In addition, the oxide of each element was used for calibration. The recorded energy step size of the spectra was varied for different regions. The pre-edge spectra were collected at a step size of 10 eV while, over the edge region, the step size was 0.25 eV with 1 s accumulation time at each step. The EXAFS region of spectra was collected at a step size of 0.04 Å⁻¹ in the k-space with 2 s accumulation time at each step. Each scan was repeated 3 times and averaged. The data processing was done using the Demeter® software package for fitting, while individual scattering paths were generated using FEFF6.

3.3.12 Electrical measurement

An LCR meter is used to measure the dielectric properties of materials by determining their electrical behavior under an applied AC signal. Dielectric properties, such as permittivity, loss tangent, and impedance, are key for characterizing insulating and capacitive materials. Impedance spectroscopy performed in LCR meter usually presented in Nyquist or Bode plots, reveals critical information about bulk conduction, grain boundary resistance, and interfacial phenomena. These measurements can also be conducted under controlled temperatures for advanced analysis. **Figure 3.15** shows the photograph of LCR

meter used to analysis of electrical properties of HEOs sample. Proper calibration of the LCR meter and considerations for minimizing contact resistance are essential for accurate results. This approach is particularly useful for characterizing dielectric properties, electrical conductivity, and ion transport behavior, which are important for applications in solid electrolytes, capacitors, and electrocatalysis. To characterize the dielectric properties and electrical conductivity the powders mixture was uniaxially pelletized into disks measuring 10 mm in diameter and 2.5 ± 0.2 mm in thickness, achieving a green density of approximately 49.27%. The green compacts were then sintered in a tube furnace (ANTS Ceramics Pvt. Ltd., India) following a two-stage heating process: an initial hold at 600 °C for 2 hours to eliminate the binder, followed by sintering at 1100 °C for 4 hours to achieve >90% relative density. Sintered pallets were coated with silver paste on both sides to make electrical contact. LCR meter (model no. E4980A/AL, Keysight, Malaysia) with a frequency range of 10 Hz to 1MHz was used to test the dielectric characteristics and perform impedance spectroscopy at three different temperatures (303 K, 363 K, and 423 K).

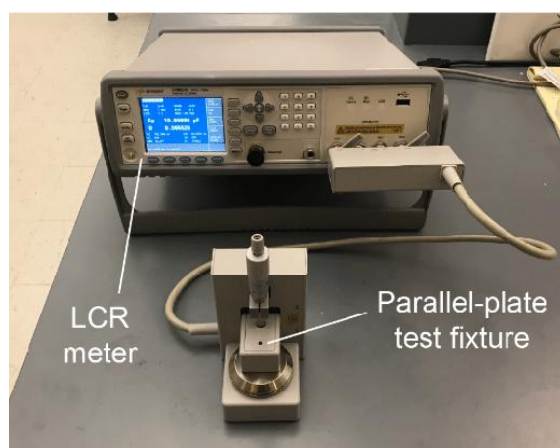


Figure 3.15 Photograph of LCR meter fitted with parallel plat test fixture.

3.3.13 Electrochemical characterization

Electrochemical characterization encompasses experimental techniques used to investigate and analyze the electrochemical behaviour of materials and systems. These techniques involve measuring and evaluating parameters such as potential, current, impedance, and charge to better understand the electrochemical processes occurring at the electrode-electrolyte interface.

Preparation of working electrode

The synthesized HEO (5 mg) sample was mixed with (2mg) graphene powder and 40 μ L of 10% Nafion solution was dispersed in 340 μ L water and 150 μ L IPA, ultrasonicated for 60 min to form a homogeneous ink. 250 μ L ink was later drop casted on cleaned carbon paper (1 cm \times 1cm) and dried in vacuum oven at 80 $^{\circ}$ C, served as the working electrode, while the Ag/AgCl electrode acted as the reference electrode, and a Pt wire was used as the counter electrode. All three electrodes were immersed in 30 mL of 1M KOH solution, which functioned as the electrolyte. For

assessing the Oxygen Evolution Reaction (OER) there are several electrochemical characterization techniques which discussed below:

Linear sweep voltameter (LSV)

Linear Sweep Voltammetry (LSV) is an electrochemical technique used to study redox reactions and analyze the electrochemical properties of materials. It involves applying a linearly varying potential to a working electrode over time while recording the resulting current. The experimental setup includes a three-electrode system which include a working electrode (where the reaction occurs), a reference electrode (to maintain a stable potential), and a counter electrode (to complete the circuit) as shown in **Figure 3.16**. As the potential sweeps through a defined range, oxidation or reduction reactions occur at the working electrode, generating a current response. This current is influenced by the kinetics of the electron transfer and the mass transport of the analyte, primarily by diffusion. The resulting voltammogram, a plot of current versus potential, typically features characteristic peaks or plateaus corresponding to redox events. Key parameters, such as redox potential, reaction kinetics, and diffusion coefficients, can be extracted from the data. The peak current is proportional to the analyte concentration, scan rate, and other factors. LSV is widely applied in identifying redox potentials, studying electron transfer kinetics, evaluating electrocatalytic activity. In our work for OER potential range applied was 1.1 to 1.9 V vs RHE.

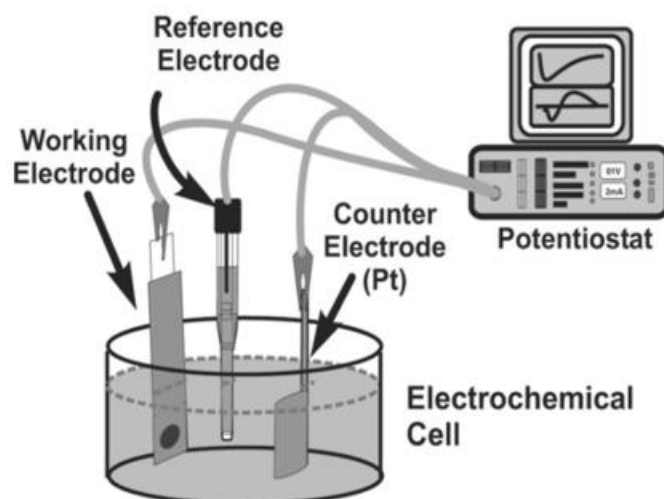


Figure 3.16 Schematic diagram of Three cell setup.

Electrochemical impedance spectroscopy (EIS)

Electrochemical Impedance Spectroscopy (EIS) is a powerful and non-invasive technique widely used to study the electrochemical behaviour of materials and interfaces. By applying a small alternating current (AC) signal to an electrochemical system and measuring the resulting voltage response, EIS provides valuable information about the system's impedance as a function of frequency. The impedance data can be used to characterize various electrochemical processes, such as charge transfer, ion diffusion, and double-layer capacitance, which are fundamental to the performance of electrochemical devices, including batteries, fuel cells, supercapacitors, and corrosion systems. EIS is a versatile tool that allows researchers to gain insights into the kinetics of electrochemical reactions, identify reaction mechanisms, and assess the performance and stability of materials under different conditions. One of the key advantages of EIS is its ability to resolve both resistive and capacitive contributions to the impedance at a range of time scales,

making it possible to study processes occurring from microseconds to seconds. The technique's sensitivity to material interfaces also makes it invaluable for analyzing electrode materials, solid-electrolyte interfaces, and corrosion phenomena. The data obtained from EIS is typically represented in Nyquist plots or Bode plots, which reveal the frequency dependence of the impedance. These plots can be fitted to equivalent circuit models, which help interpret the underlying electrochemical processes in terms of electrical components like resistors, capacitors, and inductors. This quantitative analysis is crucial for optimizing the design of electrochemical systems and understanding the effects of various factors such as temperature, electrolyte composition, and applied voltage on material performance. Overall, Electrochemical Impedance Spectroscopy offers an indispensable approach to understanding complex electrochemical systems, making it a key technique in the fields of energy storage, conversion, and corrosion protection.